4.4 LES: HOW LARGE IS LARGE ENOUGH? *

Peter G. Duynkerke, Harm J. J. Jonker [1], and Stephan R. de Roode
Institute for Marine and Atmospheric Research Utrecht, University of Utrecht, The Netherlands
[1] Dept. of Applied Physics, Delft University of Technology, The Netherlands

1. Introduction

From an analysis of the horizontal wind velocities Van der Hoven (1957) found a local minimum in the spectral energy at wavelengths in the mesoscale range. As such the concept of the 'spectral gap' was introduced, which is supposed to separate small-scale turbulent fluctuations from the larger mesoscale and synoptic perturbations. In contrast to this simple picture various field experiments performed in both clear and cloudy boundary layers have shown that there can be a significant amount of variance present at the mesoscales (Nicholls and LeMone, 1980; Young, 1987). Although the vertical velocity spectrum usually has a peak at a length scale close to the boundary layer depth, for other quantities such as moisture, temperature, or the horizontal wind components significant mesoscale contributions were found in the spectra.

Jonker et al. (1999) showed that the wavelength of the spectral peak of an arbitrary passive scalar in a convective boundary layer depends on the ratio of the surface and entrainment flux. This paper is a follow-up study of that paper. We will focus on the evolution of the length scale in clear convective and stratocumulus-topped boundary layers. To this end we have performed a Large-Eddy Simulation on a large horizontal domain (25.6x.25.6x1.6 km), which is large enough to capture the mesoscale structures. We aim to show that turbulence is capable to generate variance of passive scalars at the mesoscales.

2. Set-up of the experiment

Large-Eddy Simulations of a convective boundary layer and a stratocumulus-topped boundary layer have been performed with the IMAU/KNMI model, e.g. VanZanten (2000). The stratocumulus case is based on observations obtained at San Nicolas island in July 1987 during the FIRE I experiment. The simulations have been done with with 256 x 256 x 80 grid points. The horizontal spacing was 100 m and the vertical grid spacings were 20 m and 15, for the CBL and stratocumulus, respectively.

To diagnose the fields of an arbitrary passive scalar χ we make use of the linearity of the prognostic equation for a conserved variable which allows the application of the principle of superposition of variables (Wyngaard and Brost, 1984). We have added a bottom-up (s_{bu}) and top-down scalar (s_{td}) to the simulations. The bottom-up scalar is initialized with a constant surface flux and no concentration jump across the inversion. The top-down scalar has no surface flux but since it is initialized with a jump across the inversion a vertical flux is generated by entrainment. The vertical turbulent flux of any arbitrary quantity χ is then given by

$$\langle w'\chi'\rangle = a\langle w'\psi'\rangle + b\langle w'\phi'\rangle, \tag{1}$$

where the operator $\langle\rangle$ denotes the horizontal slab mean value. By choosing appropriate values for the factors a and b we can obtain any arbitrary flux ratio r, which is defined as the ratio of the flux of χ at the top of the boundary layer and the surface, indicated by the subscripts T and 0, respectively,

$$r = \frac{\langle w'\chi'\rangle_T}{\langle w'\chi'\rangle_0}. \tag{2}$$

Likewise the variance $\langle \chi^{'2}\rangle$ can be computed from

$$\langle \chi^{'2}\rangle = a^2\langle \psi^{'2}\rangle + b^2\langle \phi^{'2}\rangle + 2ab\langle \psi'\phi'\rangle. \tag{3}$$

The spectral characteristics of the LES generated fields in the horizontal plane are analysed from a Fourier transformation which provides a two-dimensional matrix of the (co-)spectral energy density. This spectrum is transformed to cylindrical coordinates and is subsequently integrated over all angles to give the (co)-spectrum $S_{\alpha\beta}(k)$, which satisfies

$$\langle \alpha'\beta'\rangle = \int_0^\infty S_{\alpha\beta}(k)dk \tag{4}$$

*Corresponding author address: Stephan R. de Roode, Institute for Marine and Atmospheric Research Utrecht (IMAU), Princetonplein 5, 3584 CC Utrecht, The Netherlands. Email: roode@phys.uu.nl

A convenient tool to investigate scale characteristics is the ogive. For two arbitrary quantities α and β the ogive $O_{\alpha\beta}(k)$ is defined as the integral of the spectral density between the wavenumber k and the Nyquist frequency k_{Ny} (Oncley et al., 1996),

$$O_{\alpha\beta}(k) = \int_{k}^{k_{Ny}} S_{\alpha\beta}(k)dk. \tag{5}$$

The ogive gives the contribution to the covariance made by all wavenumber components above wavenumber k. Note that $O_{\alpha\beta}(0) = \langle\alpha'\beta'\rangle$. We have computed a critical wavenumber k_c from the following expression,

$$O_{\alpha\beta}(k_c) = \frac{2}{3}\langle\alpha'\beta'\rangle. \tag{6}$$

which means that a 2/3 fraction of the cospectral energy is located between the k_c and the Nyquist wavenumber. In the majority of cases k_c is found to coincide more or less with the spectral peak, but has the advantage of being less sensitive to noise. We define the characteristic length scale Λ as,

$$\Lambda = 1/k_c. \tag{7}$$

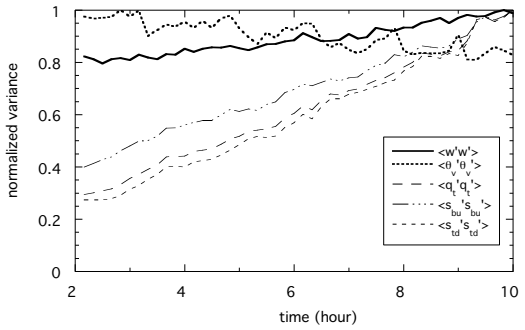

Figure 1: Variance in the middle of the convective boundary layer normalized by its maximum value for the vertical velocity, virtual potential temperature, specific humidity, and the bottom-up and top-down scalars as a function of time. The linestyles are according to the legend.

3. Results

a. The clear convective boundary layer

From the instantaneous fields at 10 minute intervals we have analyzed the variance in the middle of the boundary layer, where we took into account the gradual increase of the boundary layer depth (z_i) with time. To determine z_i we used the level of the minimum buoyancy flux. At the start of the simulation z_i is about 800 m and after 10 hours it has risen to 1040 m. During the the first two hours of simulation the turbulence in the boundary layer is still in a spin-up phase so we will not consider the results for this period. As shown in Fig. 1, the change in the variance for the vertical velocity and the virtual potential temperature, which are both dynamic quantities is rather small, as is the case for their respective characteristic length scales (see Fig. 2a). If one wants to capture a $2/3$ fraction of the variance for the vertical velocity and the virtual potential temperature in the middle of the boundary layer it suffices to consider the contributions of all eddies smaller than 1.4 and 2.0 times the BL depth z_i, respectively. In contrast, the variances for the total water content, and the bottom-up and top-down scalars increase steadily with time. A significant fraction of the variance for these quantities grows at scales much larger than the boundary layer depth, as is indicated by the their characteristic length scales which are about $5.5z_i$ after 5 hours of simulation. The disparity in the length scale behavior of scalars with a different flux ratio has already been discussed by Jonker et al. (1999). They found a minimum length scale for quantities that have a flux ratio $r \approx -0.5$. The characteristic length scales for the vertical fluxes differ for the various quantities although they are approximately constant with time.

b. Stratocumulus

Figure 3 shows an example of the time evolution of the variance for several variables in the middle of the stratocumulus-topped boundary layer. The time variation of the vertical velocity variance is small. The variances for the virtual potential temperature, the total water content and the top-down scalar tend to increase with time. As shown in Fig. 4a the characteristic length scale for the vertical velocity variance is larger than for the CBL, $\Lambda_{\langle w^2\rangle} = 2.6z_i$. The fact that there are more vertical fluctuations present at the larger scales has an important consequence. The characteristic length scales for the fluxes and variances for θ_v, q_t, s_{td} and s_{bu} grow considerably faster with time indicating an increasing importance of fluctuations on the mesoscales.

4. Discussion

We have shown that mesoscale fluctuations develop in both clear and cloudy boundary layers. It should be stressed that for the CBL this can only be attributed to turbulence, since there are no other external forcings present. The production of variance for χ (P_{χ^2}) is pro-

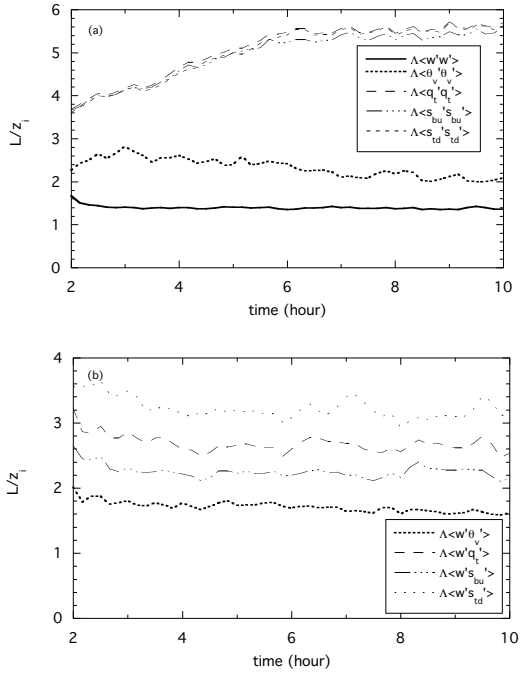

Figure 2: Length scale normalized by the boundary layer depth in the middle of the convective boundary layer as a function of time. (a) Variances. (b) Fluxes.

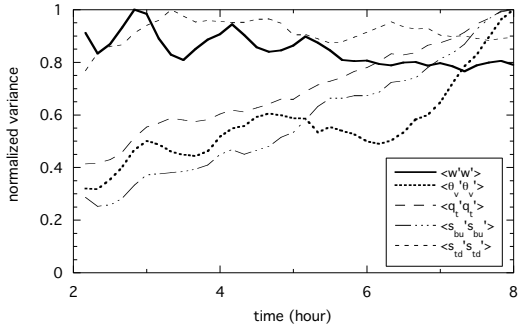

Figure 3: Variance in the middle of the stratocumulus-topped boundary layer normalized by its maximum value as a function of time.

portional to the vertical flux multiplied times the mean vertical gradient,

$$P_{\chi^2} = -2\langle w'\chi'\rangle \frac{\partial\langle\chi\rangle}{\partial z}. \qquad (8)$$

Hence, variance will be produced at all scales where there is a vertical flux and a vertical mean gradient that has an opposite sign to the flux. Fig. 5a clearly shows the dominance of mesoscale fluctuations in the CBL for the bottom-up and top-down scalars, which must be produced by the (weak) vertical fluxes at the largest scales

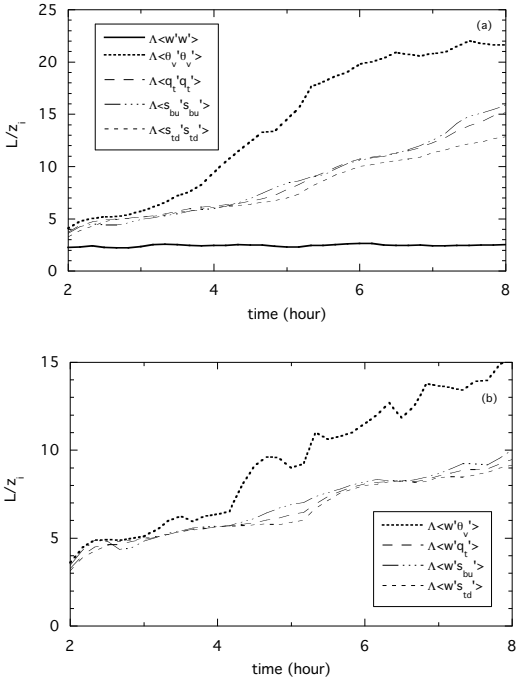

Figure 4: Scaled length scale evolution in the middle of the stratocumulus-topped boundary layer as a function of time. (a) Variance. (b) Flux.

(shown in the middle panel).

For the stratocumulus case mesoscale fluctuations develop for all flux ratios. In contrast to this finding, in the CBL the contribution of the mesoscales to the total variance is only minimal for flux ratios near $r = -0.2$, which is a typical value for the buoyancy. The energy spectra can shed some light on the question why the buoyancy variance does only exhibit a minimum amount of fluctuations at the mesoscales. The virtual potential temperature energy spectrum can be obtained from the spectral equivalent of (3). Since both the bottom-up and top-down scalars contribute to mesoscale fluctuations when added according to (3), a negative value for the correlation term $2ab\langle\psi'\phi'\rangle$ can explain the relatively small amount of mesoscale fluctuations for the buoyancy. Thus, for the buoyancy mesoscale fluctuations induced separately by the surface and entrainment fluxes are partly offset.

If there is no windshear, the buoyancy flux is the major production term for the vertical velocity variance (P_{w^2}). Therefore, the production terms in the prognostic equations for $\langle\theta_v'^2\rangle$ and $\langle w'^2\rangle$ are related as,

$$P_{w^2} = 2\frac{g}{\theta_0}\langle w'\theta_v'\rangle = -\frac{g}{\theta_0}\left(\frac{\partial\langle\theta_v\rangle}{\partial z}\right)^{-1} P_{\theta_v^2}. \qquad (9)$$

Eq. (9) indicates that if the BL is unstably stratified the production terms for $\langle \theta_v^{'2} \rangle$ and $\langle w^{'2} \rangle$ act to generate fluctuations simultaneously. Fiedler and Khairoutdinov (1994) have reported that for a BL with a constant buoyancy flux mesoscale fluctuations in $\langle \theta_v^{'2} \rangle$ grow rapidly. For this case the bulk of the BL is unstably stratified. However, note that the continuity equation prevents an unlimited growth of mesoscale fluctuations in the vertical velocity. Entrainment of warm air from above the inversion, which acts to stabilize the upper part of the CBL, may be the reason that the mesoscale fluctuations for the buoyancy are only minimal. In contrast, in the simulation of a smoke cloud, in which the boundary layer is uniformly cooled by longwave radiation at the top, we also found a gradual growth of mesoscale fluctuations for the buoyancy. Since a smoke cloud does not contain liquid water droplets this can not be explained by latent heat release due to condensation. Since the flux ratios for the buoyancy differ for the smoke cloud and the CBL, it seems that this ratio is of key importance for the generation of mesoscale fluctuations.

Acknowledgement The investigations were supported by the Netherlands Organization for Scientific Research (NWO). This work was sponsored by the National Computing Facilities Foundation (NCF) for the use of supercomputer facilities.

References

Fiedler, B. H. and M. Khairoutdinov, 1994: Cell broadening in three-dimensional thermal convection between poorly conducting boundaries. *Beitr. Phys. Atmos.*, **51**, 1114–1119.

Jonker, H. J. J., P. G. Duynkerke, and J. W. M. Cuijpers, 1999: Mesoscale fluctuations in scalars generated by boundary layer convection. *J. Atmos. Sci.*, **56**, 801–808.

Nicholls, S. and M. A. LeMone, 1980: The fair weather boundary layer in GATE: The relation of subcloud fluxes and structure to the distribution and enhancement of cumulus clouds. *J. Atmos. Sci.*, **37**.

Oncley, S., C. Friehe, J. Larue, J. Businger, E. Itsweire, and S. S. Chang, 1996: Surface-layer fluxes, profiles, and turbulence measurements over uniform terrain under near-neutral conditions. *J. Atmos. Sci.*, **53**, 1029–1044.

Van der Hoven, I., 1957: Power spectrum of horizontal wind speed in the frequency range from 0.0007 to 900 cycles per hour. *J. Meteor.*, **14**, 160–164.

VanZanten, M. C., 2000: *Entrainment processes in stratocumulus*. Ph.D. thesis, Utrecht University, Utrecht, 139 pp (Available from Utrecht University, Utrecht, The Netherlands).

Wyngaard, J. C. and R. A. Brost, 1984: Top-down and bottom-up diffusion of a scalar in the convective boundary layer. *J. Atmos. Sci.*, **41**, 102–112.

Young, G. S., 1987: Mixed layer spectra from aircraft measurements. *J. Atmos. Sci.*, **44**, 1251–1256.

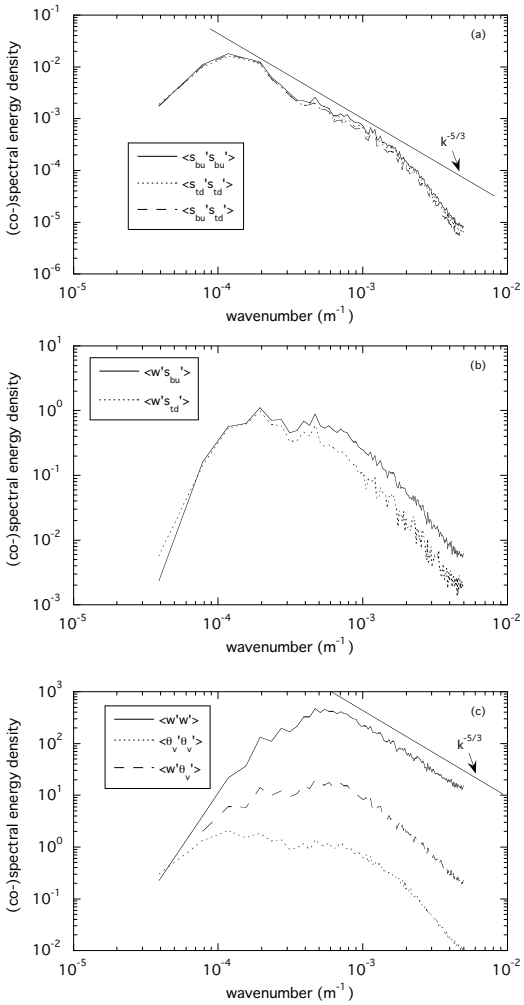

Figure 5: Energy spectra as a function of the wavenumber in the middle of the convective boundary layer after 10 hours of simulation. (a) The bottom-up and top-down scalars and their cospectrum. (b) Co-spectral energy of the bottom-up and top-down fluxes. (c) The vertical velocity, the virtual potential temperature variance, and their cospectrum. The straight line indicates a $-5/3$ slope.